On Excitation of Zonal Structures by Kinetic Alfvén Waves

L. Chen[1,2], F. Zonca[3,1] and Y. Lin[4]

[1]Institute for Fusion Theory and Simulation and Dept. of Physics, Zhejiang University, Hangzhou 310027, P.R.C.
[2]Dept. of Physics and Astronomy, Univ. of California, Irvine CA 92697-4575, U.S.A.
[3]C.R. ENEA Frascati - C.P. 65, 00044 Frascati, Rome, Italy
[4]Physics Dept., Auburn University - Auburn, AL 36849-5311, USA

Corresponding Author: liuchen@zju.edu.cn

Abstract:
Zonal flow (ZF) and zonal current (ZC) in fusion devices are manifestations of, respectively, electrostatic (ESCC) and magnetostatic (MSCC) convective cells in uniform plasmas. Similarly, kinetic Alfvén waves (KAW) appear as kinetic Alfvén eigenmodes (KAE) due to the presence of Alfvén continuum. Employing this paradigm, we have investigated the spontaneous excitation of CC via modulational instabilities induced by a finite-amplitude pump KAW both analytically and by numerical simulations. Our results demonstrate that kinetic finite ion Larmor radius (FILR) effects play crucially important roles in the excitation mechanism. More specifically, we have found that (i) spontaneous excitation only sets in when both the pump KAW and the CC have perpendicular wavelengths comparable to the ion Larmor radius, and (ii) both ESCC (ZF) and MSCC (ZC) are excited simultaneously. Results of fluid-electron and Vlasov-ion hybrid simulations show good agreements with analytical predictions. Implications to ZF/ZC excitations by KAEs in laboratory fusion devices will also be discussed.

1 Introduction

In magnetically confined fusion plasmas such as tokamaks, zonal flows (ZF) and zonal currents (ZC) or, more generally, zonal structures (ZS) correspond to long-lived or oscillating electromagnetic perturbations with predominant variations in the radial direction. Since, typically, ZS are linearly stable, they are usually nonlinearly excited via mode-mode coupling processes by the primary driving waves such as drift-wave or Alfvén wave instabilities [1]. As ZS have micro-scale (ρ_i) or meso-scale ($\sqrt{\rho_i a}$) radial variations, they may be regarded as radial corrugations in the macro-scale (a) "smooth" equilibrium parameters. Here, ρ_i and a are, respectively, the thermal ion Larmor radius and the minor radius of, e.g., a tokamak plasma. Thus, as the secondary ZS are nonlinearly excited, they will scatter the primary driving instabilities to shorter-wavelength stable regime and, thereby, nonlinearly stabilize the driving instabilities. In addition, the electromagnetic ZS

perturbations could also modify charged-particle phase-space orbits. As a consequence, wave-particle resonance could be detuned; leading to suppression of the instability driving mechanism. That ZS could play crucial roles in self-regulating the nonlinear evolution of the driving instabilities and associated plasma transport processes have motivated intensive research on this topic by the fusion community.

Shear Alfvén waves (SAW), manifested as Alfvén eigenmodes (AEs) spontaneously excited by various instabilities, are prevalent in magnetically confined fusion devices [2]. It is, therefore, important to understand the nonlinear generating mechanisms of ZS by SAW. Previous studies have revealed an important property of ZS generation by SAW. That is, in the long-wavelength ideal magnetohydrodynamic (MHD) regime, the two dominant nonlinear wave coupling processes, the Reynolds and Maxwell stresses, cancel each other [3, 4]; leading toward the existence of the so-called Alfvénic state [5, 6]. In order to investigate ZS generation by SAW, one, thus, needs to break the Alfvénic state by considering effects due to, e.g., the toroidal geometry and/or the finite ion Larmor radii (FILR) [7]. In the latter regime, SAW becomes the kinetic Alfvén wave (KAW) and is the focus of the present investigations. Note that, in fusion devices, KAWs appear as kinetic AEs (KAEs) due to the presence of SAW continuum.

In the present work, we address the modulational instability process by which KAW may excite convective cells (CC) in a uniform magnetized plasma. As shown below, this is a useful paradigm to elucidate ZS generation by KAW through the braking of the Alfvénic state at short wavelength. Modulational instability, in general, is the reinforcement by nonlinearity of the deviation from wave periodic behavior, which may lead to spectral sidebands and possibly to breaking of the periodic fluctuation into modulated pulses. In Sec. 2, we present the theoretical framework for the analysis of modulational instability of a finite amplitude KAW and its decay into CCs and matching sideband KAWs. This allows us to derive the dispersion relation of modulational instability and the threshold condition for CC excitation. To verify analytical predictions, Sec. 3 illustrates numerical analyses obtained by a hybrid code solving for responses of fully kinetic ions and massless electron fluid [8, 9]. Numerical simulation results and analytical theory are shown to be in excellent agreement [10]. Finally, Sec. 4 provides concluding remarks and a discussion of the implications of present results for ZS generation by KAE in toroidal fusion plasmas.

2 Theoretical formulation

Convective cells are zero-frequency electromagnetic perturbations, which vary only perpendicular to the confining magnetic field $\boldsymbol{B}_0$; i.e., with parallel wave number $k_\parallel = \boldsymbol{k} \cdot \boldsymbol{B}_0/B_0 = 0$. Zero-frequency ZS (ZFZS), thus, can be considered as a manifestation of CC in laboratory fusion devices. In particular, zonal flow (ZF) and zonal current (ZC) correspond to electrostatic (ESCC) and magnetostatic (MSCC) convective cells, respectively. The adopted theoretical model then consists of modulational interactions between a finite-amplitude pump KAW, $(\omega_0, \boldsymbol{k}_0)$, and small-amplitude electromagnetic CC, $(\omega_z, \boldsymbol{k}_z)$, as well as lower- and upper-KAW sidebands; ($\omega_- = \omega_z - \omega_0$, $\boldsymbol{k}_- = \boldsymbol{k}_z - \boldsymbol{k}_0$, $\omega_+ = \omega_z + \omega_0$, $\boldsymbol{k}_+ = \boldsymbol{k}_z + \boldsymbol{k}_0$). Here, ω_0 and $\boldsymbol{k}_0$ satisfy the linear KAW dispersion relation

and $k_{\|z}=0$. The perturbed distribution functions are given by the nonlinear gyrokinetic equation [11]; i.e.,

$$\delta f_k = -\left(e/T\right) F_M \delta\phi_k + \exp\left(-i\boldsymbol{\rho}\cdot\boldsymbol{k}_\perp\right)\delta g_k \ , \tag{1}$$

$$i\left(k_\parallel v_\parallel - \omega_k\right)\delta g_k - (c/B_0)\Lambda^{k''}_{k'}\left[\langle\delta L_g\rangle_{k'}\,\delta g_{k''} - \langle\delta L_g\rangle_{k''}\,\delta g_{k'}\right] = -i\omega_k\left(e/T\right)F_M\,\langle\delta L_g\rangle_k \ . \tag{2}$$

Here, $\boldsymbol{B}_0 = B_0\hat{\boldsymbol{z}}$, F_M is the Maxwellian distribution, $\boldsymbol{\rho}=\hat{\boldsymbol{z}}\times\boldsymbol{v}/\Omega$, $\Omega = eB_0/(mc)$, $\Lambda^{k''}_{k'} = (\boldsymbol{k}'_\perp\times\boldsymbol{k}''_\perp)\cdot\hat{\boldsymbol{z}}$, $\boldsymbol{k}=\boldsymbol{k}'+\boldsymbol{k}''$, $\langle ...\rangle$ denotes gyro-phase averaging, $\delta L_g = \exp\left(\boldsymbol{\rho}\cdot\boldsymbol{\nabla}\right)\delta L$, $\delta L = \delta\phi - v_\parallel\delta A_\parallel/c$ and $\langle\delta L_g\rangle_k = J_k\left(\delta\phi - v_\parallel\delta A_\parallel/c\right)_k \equiv J_k\delta L_k$. $\delta\phi$ and $\delta A_\parallel$ are, respectively, the scalar and the parallel to $\boldsymbol{B}_0$ component of the vector potentials, $J_k = J_0(k_\perp\rho)$ with J_0 the Bessel function and $\rho = v_\perp/\Omega$. Meanwhile, the field equations are given by the following quasi-neutrality condition, which, assuming one single ion species with unit electric charge and n_0 equilibrium density, becomes

$$\left(1+T_i/T_e\right)\delta\phi_k = T_i/(n_0 e)\int\left(J_k\delta g_{ki} - \delta g_{ke}\right)d\boldsymbol{v} \ , \tag{3}$$

along with the generalized nonlinear gyrokinetic vorticity equation

$$\begin{aligned} ik_\parallel\delta j_{\parallel k} \ - \ i\frac{c^2}{4\pi}\frac{\omega_k k_\perp^2}{v_A^2 b_k}(1-\Gamma_k)\delta\phi_k = -\Lambda^{k''}_{k'}\left(\delta A_{\parallel k'}\frac{\delta j_{\parallel k''}}{B_0} - \delta A_{\parallel k''}\frac{\delta j_{\parallel k'}}{B_0}\right) \\ +\frac{ec}{B_0}\Lambda^{k''}_{k'}\int[(J_kJ_{k'}-J_{k''})\delta L_{k'}\delta g_{k''i} - (J_kJ_{k''}-J_{k'})\delta L_{k''}\delta g_{k'i}]d\boldsymbol{v}. \end{aligned} \tag{4}$$

Here, $\Gamma_k = I_0(b_k)\exp(-b_k)$, I_0 is the modified Bessel function, $b_k = k_\perp^2\rho_i^2$, the Alfvén speed is $v_A = B_0/(4\pi n_0 m_i)^{1/2}$, and $\delta j_{\|k}$ is given by the Ampère's law $\delta j_{\|k} = (c/4\pi)k_\perp^2\delta A_{\|k}$. The first nonlinear term on the right hand side of Eq. (4) is the Maxwell stress, while the second one reduces to the well-known Reynolds stress for $b_k \ll 1$ [2, 10].

Equations (3) and (4) can be thought of, respectively, as equation for $\delta\phi_k$ and $\delta\psi_k \equiv \omega_k\delta A_{\|k}/(k_\|c)$, which we choose as field variables. Thus, Eqs. (3) and (4) fully determine the nonlinear evolution of $k_\| \neq 0$ modes, that is of KAW sidebands, while the pump KAW satisfies the linear mode dispersion relation

$$\epsilon_{Ak}|_{\boldsymbol{k}=\boldsymbol{k}_0} = \left[\frac{1-\Gamma_k}{b_k} - \sigma_k\frac{k_\parallel^2 v_A^2}{\omega_k^2}\right]_{\boldsymbol{k}=\boldsymbol{k}_0} = 0 \ , \tag{5}$$

with $\sigma_k \equiv 1+\tau(1-\Gamma_k)$, $\tau\equiv T_e/T_i$; and the polarization condition $\delta\psi_0 = \sigma_0\delta\phi_0$. For $k_\| = 0$ CC modes, Eqs. (3) and (4) are not independent [2, 10]: Eq. (4) can be used for the ESCC response $\delta\phi_z$, while the equation for the MSCC response $\delta\psi_z \equiv \omega_0\delta A_{\|z}/(k_{\|0}c)$ is given by the parallel electron force balance, which can be suitably rewritten as [10]

$$\delta\psi_z = i\frac{c\sigma_0}{\omega_0 B_0}\Lambda^{k_z}_{k_0}\left(\frac{\delta\phi_0\delta\psi_-}{1-\omega_z/\omega_0} + \frac{\delta\phi_0^*\delta\psi_+}{1+\omega_z/\omega_0}\right) \ . \tag{6}$$

Employing the above equations, one can then straightforwardly derive an analytical KAW-CC modulational instability dispersion relation, which depends on parameters such

as $\boldsymbol{k}_0 = k_{\|0}\hat{\boldsymbol{z}} + k_x\hat{\boldsymbol{x}}$, $\boldsymbol{k}_z = k_y\hat{\boldsymbol{y}}$ and the pump amplitude δB_y. In particular, Eqs. (3) and (4) are solved for the KAW sideband response, $\delta\phi_\pm$ and $\delta\psi_\pm$, which is then substituted into the CC response; i.e., Eq. (4) for $\delta\phi_z$ and Eq. (6) for $\delta\psi_z$. The modulational instability dispersion relation can be derived in general, but below we specialize to the case $\boldsymbol{k}_z \perp \boldsymbol{k}_{\perp 0}$ in order to maximize nonlinear interaction. Thus, $b_\pm = b_0 + b_z$, $\Gamma_+ = \Gamma_-$, etc.; and the frequency mismatch, $\Delta_\pm = \Delta$, of KAW sidebands with respect to normal mode frequency is [10]

$$\frac{\Delta}{\omega_0} = \frac{b_+\sigma_+(1-\Gamma_0) - b_0\sigma_0(1-\Gamma_+)}{2b_0\sigma_0(1-\Gamma_+)} \,. \tag{7}$$

In this way, letting $\omega_z = i\gamma_z$, the coupled nonlinear equations for CC response can be cast as [10]

$$\begin{aligned}
\left[\gamma_z^2 + \frac{\Delta^2}{1+\Delta/\omega_0} + \frac{\gamma_z^4}{4\omega_0^2(1+\Delta/\omega_0)}\right]\delta\phi_z &= -\alpha_\phi(\delta\phi_z - \delta\psi_z) + \beta_\phi\delta\psi_z \\
&\quad + \frac{\gamma_z^2}{2\omega_0^2(1+\Delta/\omega_0)}\left[-\hat{\alpha}_\phi(\delta\phi_z - \delta\psi_z) + \hat{\beta}_\phi\delta\psi_z\right] \,, \\
\left[\gamma_z^2 + \frac{\Delta^2}{1+\Delta/\omega_0} + \frac{\gamma_z^4}{4\omega_0^2(1+\Delta/\omega_0)}\right]\delta\psi_z &= -\alpha_\psi(\delta\phi_z - \delta\psi_z) + \beta_\psi\delta\psi_z \\
&\quad + \frac{\gamma_z^2}{2\omega_0^2(1+\Delta/\omega_0)}\left[-\hat{\alpha}_\psi(\delta\phi_z - \delta\psi_z) + \hat{\beta}_\psi\delta\psi_z\right] \,.
\end{aligned} \tag{8}$$

Here, the nonlinear couplings are controlled via [10]

$$\begin{aligned}
\alpha_\phi &= \left|\frac{c}{B_0}k_z k_{\perp 0}\delta\phi_0\right|^2 \frac{1}{1-\Gamma_+}\left[\frac{\Gamma_0-\Gamma_+}{1-\Gamma_z}\left(\Gamma_0 - \Gamma_z - \frac{b_+}{b_0}\frac{1-\Gamma_0}{1+\Delta/\omega_0}\right)\right. \\
&\quad \left. + \frac{b_z(1-\Gamma_0)}{b_0(1-\Gamma_z)}\left((1-\Gamma_+)\,\sigma_0 - \frac{(\Gamma_0-\Gamma_z)\,\sigma_+}{1+\Delta/\omega_0}\right)\right] \,, \\
\beta_\phi &= \left|\frac{c}{B_0}k_z k_{\perp 0}\delta\phi_0\right|^2 \frac{1}{1-\Gamma_+}\left[\frac{b_z(1-\Gamma_0)}{b_0(1-\Gamma_z)}\frac{\sigma_+}{1+\Delta/\omega_0} - \frac{\Gamma_0-\Gamma_+}{1-\Gamma_z}\right]\left(1-\Gamma_z - b_z\frac{1-\Gamma_0}{b_0}\right) \,, \\
\hat{\alpha}_\phi &= \left|\frac{c}{B_0}k_z k_{\perp 0}\delta\phi_0\right|^2 \frac{1}{1-\Gamma_+}\left[\frac{\Gamma_0-\Gamma_+}{1-\Gamma_z}(\Gamma_0-\Gamma_z) + \frac{b_z(1-\Gamma_0)}{b_0(1-\Gamma_z)}(1-\Gamma_+)\,\sigma_0\right] \,, \\
\hat{\beta}_\phi &= -\left|\frac{c}{B_0}k_z k_{\perp 0}\delta\phi_0\right|^2 \frac{1}{1-\Gamma_+}\left(\frac{\Gamma_0-\Gamma_+}{1-\Gamma_z}\right)\left(1-\Gamma_z - b_z\frac{1-\Gamma_0}{b_0}\right)
\end{aligned}$$

Meanwhile [10],

$$\begin{aligned}
\alpha_\psi &= \left|\frac{c}{B_0}k_z k_{\perp 0}\delta\phi_0\right|^2 \frac{\sigma_0}{1-\Gamma_+}\frac{\Delta/\omega_0}{1+\Delta/\omega_0}\left[(1-\Gamma_+)\,\sigma_0 - (\Gamma_0-\Gamma_z)\,\sigma_+\right] \,, \\
\beta_\psi &= \left|\frac{c}{B_0}k_z k_{\perp 0}\delta\phi_0\right|^2 \frac{\sigma_0}{1-\Gamma_+}\frac{\Delta/\omega_0}{1+\Delta/\omega_0}\sigma_+\left(1-\Gamma_z - b_z\frac{1-\Gamma_0}{b_0}\right) \,,
\end{aligned}$$

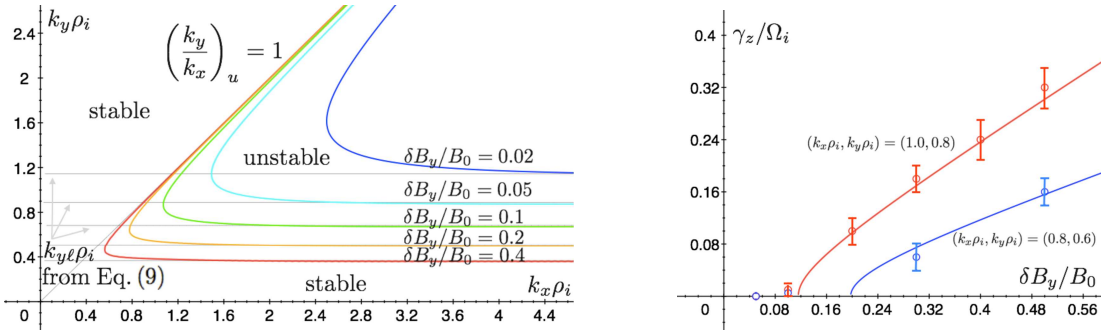

FIG. 1: (left) Marginal stability curves in the $(k_x\rho_i, k_y\rho_i)$ plane for fixed $k_{\|0}\rho_i = 0.02$, $\tau = 1$ and $\beta_e = \beta_i = 0.2$ and different values of $\delta B_y/B_0$. (right) Modulational instability growth rate (continuous line) vs. $\delta B_y/B_0$ is compared with hybrid simulation results (open circles) for $(k_x\rho_i, k_y\rho_i) = (0.8, 0.6)$ (blue) and $(k_x\rho_i, k_y\rho_i) = (1.0, 0.8)$ (red). [Reproduced and adapted from Ref. [10].]

$$\hat{\alpha}_\psi = -\left|\frac{c}{B_0}k_z k_{\perp 0}\delta\phi_0\right|^2 \frac{\sigma_0}{1-\Gamma_+}\left[(1-\Gamma_+)\,\sigma_0 + (\Gamma_0 - \Gamma_z)\,\sigma_+\right] ,$$
$$\hat{\beta}_\psi = \left|\frac{c}{B_0}k_z k_{\perp 0}\delta\phi_0\right|^2 \frac{\sigma_0\sigma_+}{1-\Gamma_+}\left(1 - \Gamma_z - b_z\frac{1-\Gamma_0}{b_0}\right) .$$

Note that Eqs. (8) are valid in general for finite $\gamma_z/\omega_0 \sim \mathcal{O}(1)$ and $\Delta/\omega_0 \sim \mathcal{O}(1)$.

The dispersion relation reveals an interesting property of marginal stability; that is, the threshold amplitude increases sharply as $|k_x\rho_i|$ or $|k_z\rho_i|$ become small. In fact, one can demonstrate analytically that, for $|k_x\rho_i| \ll 1$, the modulational instability is always stable. The instability, thus, sets in only when both the pump KAW and CC are in the short wavelength regime. Marginal stability curves in the $(k_x\rho_i, k_y\rho_i)$ plane are shown in FIG. 1 (left) for fixed $k_{\|0}\rho_i = 0.02$, $\tau = 1$ and $\beta_e = \beta_i = 0.2$ and different values of $\delta B_y/B_0$. Analytically, it is possible to show that the upper boundary of the unstable domain is given by $(k_y/k_x)_u = 1$, while the lower boundary can be obtained from the condition on $b_{z\ell} = k_{y\ell}^2\rho_i^2$ [10]

$$\frac{b_{z\ell}(1-\Gamma_{z\ell})}{2\Gamma_{z\ell} - \tau(1-\Gamma_{z\ell})} = \frac{4k_{\|0}^2\rho_i^2}{|\delta B_y/B_0|^2} . \tag{9}$$

3 Kinetic ion – fluid electron hybrid numerical simulations

To verify the analytical predictions, discussed above, we have further carried out numerical simulations using a hybrid code consisting of massless electrons and fully kinetic ions [8, 9]. The growth rates measured in simulations agree well with those predicted analytically.

Simulations also demonstrate that the excited CCs are electromagnetic in nature; i.e., both ESCC (zonal flow) and MSCC (zonal current) are excited simultaneously.

The simulation scheme is fully nonlinear and similar to that of *Lin, Johnson, ad Wang* [8, 9], in which ions are treated as fully kinetic particles moving in a self-consistent electromagnetic field, and electrons are treated as a massless fluid. In the present application, however, our analysis of the modulational instability focuses only on the early linear stage of its exponential growth. The investigation of the fully nonlinear evolution of the system after ESCC and MSCC are excited by KAW modulational instability is beyond the scope of our analysis and requires further studies.

Fixed parameters are those of FIG. 1 (left), lengths are normalized to ρ_i, and the time to Ω_i^{-1}. The pump mode is imposed everywhere as a steady driver with $\delta\boldsymbol{B}_0 = (0, \delta B_y, 0)\sin(\omega_0 t - k_x x - k_{\|0} z)$ and specified wave number and frequency, which are consistent with linear KAW polarization condition and mode dispersion relation [10]. In what follows, $\omega_0 > 0$ and $k_{\|0} > 0$ are assumed without loss of generality. From $t =$ 0-10, the system is filtered to keep only the Fourier mode $\boldsymbol{k}_0$ of initial pump, which allows a self-consistently development of the pump field structure. For $t > 10$, more Fourier modes are released in order to examine the excitation of the CC modes $\boldsymbol{k}_z = (0, k_y, 0)$ and the matching KAW sidebands due to couplings of pump KAW with CC modes. Theoretically derived modulational instability growth rate (continuous line) vs. $\delta B_y/B_0$, based on Eqs. (8), is compared with hybrid simulation results (open circles) for $(k_x\rho_i, k_y\rho_i) = (0.8, 0.6)$ (blue) and $(k_x\rho_i, k_y\rho_i) = (1.0, 0.8)$ (red) in FIG. 1 (right). Error bars on numerical growth rates are mostly due to discrete particle noise in the simulations. FIG. 2, meanwhile, shows the time evolution of δB_y, δB_x, and δE_y in the resulting three wave interaction for a case with constant pump amplitude $\delta B_y/B_0 = 0.5$ at $\boldsymbol{k}_0 = (0.8, 0, 0.02)$. The black solid curves show the pump mode, for which δB_y is constant in time. The δE_y component of the pump is two orders of magnitude smaller than δE_x (not shown). The excitation of the CC mode, with wave number $\boldsymbol{k}_z = (0, 0.6, 0)$, is shown with the red curve. Both δB_x and δE_y increase nearly exponentially with time from $t = 10$, as fitted by the straight dotted line, reaching the saturation levels at $t \simeq 53$. The growth rate is measured to be $\gamma_z/\Omega_i = 0.16$. No power is excited in the δB_y component, consistent with $k_x = 0$ in the CC mode. The green curve depicts the matching KAW mode with $\boldsymbol{k}_+ = (0.8, 0.6, 0.02)$, in which δB_x, δB_y, and δE_y are all seen to also grow exponentially with $\gamma_z/\Omega_i = 0.16$.

4 Discussions and Conclusions

The present work suggests that filamentary structures including inductive $\delta E_\|$ with $|k_\|\rho_i| = 0$ and $|k_\perp\rho_i| \sim \mathcal{O}(1)$ can be efficiently generated by CC spontaneous emission from KAW [10]. This process can operate simultaneously and, generally, is in direct competition with KAW parametric decay into sound wave and back-scattered KAW [7, 9, 12]. Thus, the results presented in this work stress the crucial importance of kinetic analyses for the proper qualitative and quantitative prediction of nonlinear behaviors of Alfvénic fluctuations in uniform plasmas [2, 7]. The corresponding self-consistent nonlinear evolution remains unexplored, with possible implications on vortex and/or current filaments formation. Such

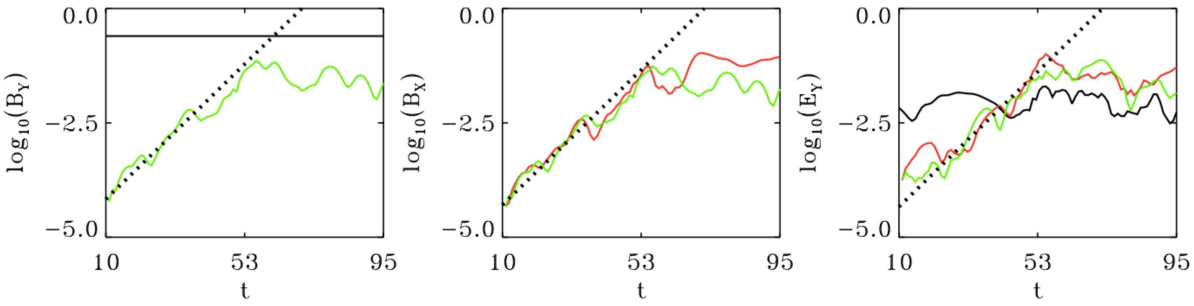

FIG. 2: Time evolution of δB_y, δB_x, and δE_y in the pump KAW (black), daughter CC (red), and the matching KAW (green). [Reproduced from Ref. [10].]

studies require fully nonlinear simulations and (gyro-)kinetic analyses [10].

The present results have significant implications on cross field transport. In fact, the linear phase of the modulational instability, which underlies spontaneous CC excitation by KAW, tends to isotropize the perpendicular KAW spectrum as a consequence of the condition $\boldsymbol{k}_z \perp \boldsymbol{k}_{\perp 0}$ for maximization of the CC generation rate. Thus, when the initial KAW spectrum is strongly anisotropic in the radial direction due to mode conversion at SAW resonances at the magnetopause [8, 9], perpendicular transport can occur only after isotropization of KAW $\boldsymbol{k}_\perp$-spectrum toward the East-West longitudinal direction via spontaneous CC excitation.

In fusion devices, as anticipated above, KAWs appear as kinetic AEs (KAEs) due to the presence of SAW continuum. Similar to KAW near the magnetopause, KAE spectrum in toroidal fusion plasmas is strongly anisotropic in the radial direction [2]; and generation of ZS by KAE modulational instability, with both ZF and ZC components, isotropizes the fluctuation spectrum with significant implications on cross field transport. The present results in uniform plasmas are, thus, readily extended to toroidal fusion plasmas [10].

Generation of ZS by KAEs in fusion devices also has a crucial role as regulation of fluctuation induced transport. In fact, as anticipated earlier, ZS are linearly stable and typically scatter the primary driving instabilities to the shorter-wavelength stable domain, acting as saturation mechanism for the KAE fluctuation spectrum. Meanwhile, due to the important role of resonant energetic particles (EPs) in the excitation of Alfvénic fluctuation in fusion plasmas [2], ZS may generally have a counterpart in the phase space and exist as phase space zonal structures (PSZS) [13]. Further to this, ZS/PSZS due to KAE may have micro- and meso-scales characterized by both thermal plasma as well as EP FILR. Thus, they can effectively act as cross-scale coupling between fluctuations on disparate spatiotemporal scales [14].

To properly assess ZS generation in toroidal fusion plasmas by KAE modulational instability, it is crucial to understand the processes underlying the breaking of the Alfvénic state [7, 10]. In addition to FILR, discussed above for uniform plasmas, the additional twist of complex geometry can also importantly modify the properties of the SAW continuous spectrum and mode converted KAW in fusion devices [2]. In particular, frequency gaps in the SAW continuum ultimately break the cancelation of Reynolds and Maxwell

stresses [15]. Finite plasma compressibility also has an important role in breaking the Alfvénic state [2, 7]. Due to modified particle orbits in toroidal geometry, and due to the unique role of geodesic curvature in causing enhanced radial particle drifts, there is a complex interplay of FILR, geometry, plasma compressibility and finite magnetic drift orbit widths that must be taken into account for a proper analysis of nonlinear Alfvén wave physics in toroidal fusion plasmas [16, 17, 18]. Thus, nonlinear generation of ZS must be carried out bearing in mind that nonlinear gyrokinetic analyses in realistic magnetic equilibria are generally needed to provide an accurate and realistic description of fusion devices [2, 10, 13, 14].

Acknowledgments

This work was supported by NMCFERP-CN, US DoE, NSF, NSFC and EUROfusion Consortium grants.

References

[1] DIAMOND, P. H., et al., Plasma Phys. Control. Fusion **47** (2005) R35.
[2] CHEN, L., and ZONCA, F., Rev. Mod. Phys. **88** (2016) 015008.
[3] ALFVÉN, H., "Cosmical Electrodynamics" (Clarendon, Oxford, UK) 1950.
[4] ELSASSER, W. M., Rev. Mod. Phys. **28** (1956) 135.
[5] ALFVÉN, H., Nature **150** (1942) 405.
[6] WALÉN, C., Ark. Mat. Astron. Fys. **30A** (1944) 1.
[7] CHEN, L., and ZONCA, F., Phys. Plasmas **20** (2013) 055402.
[8] LIN, Y., et al., J. Geophys. Res. **115** (2010) A04208.
[9] LIN, Y., et al., Phys. Rev. Lett. **109** (2012) 125003.
[10] ZONCA, F., LIN, Y., and CHEN, L., Europhys. Lett. **112** (2015) 65001.
[11] FRIEMAN, E. A., and CHEN, L., Phys. Fluids **25** (1982) 502.
[12] CHEN, L., and ZONCA, F., Europhys. Lett. **96** (2011) 35001.
[13] ZONCA, F., et al., New J. Phys. **17** (2015) 013052.
[14] ZONCA, F., et al., Plasma Phys. Control. Fusion **57** (2015) 014024.
[15] CHEN, L., and ZONCA, F., Phys. Rev. Lett. **109** (2012) 145002.
[16] QIU, Z., CHEN, L., and ZONCA, F., Nucl. Fusion **56** (2016) 106013.
[17] QIU, Z., CHEN, L., and ZONCA, F., Phys. Plasmas **23** (2016) 090702.
[18] QIU, Z., CHEN, L., and ZONCA, F., "Nonlinear Zonal Structure Generation by Toroidal Alfvén Eigenmode", 26th IAEA Fusion Energy Conference, Kyoto, 17 - 22 October 2016, Poster TH/P4-21.